Available online at www.sciencedirect.com
SCIENCE DIRECT®
Journal of Solid State Chemistry 177 (2004) 4564–4568
JOURNAL OF SOLID STATE CHEMISTRY
www.elsevier.com/locate/jssc

Influence of the structure on electric and magnetic properties of $La_{0.8}Na_{0.2}Mn_{1-x}Co_xO_3$ perovskites

E. Pollert[a,*], J. Hejtmánek[a], Z. Jirák[a], K. Knížek[a], M. Maryško[a], J.P. Doumerc[b], J.C. Grenier[b], J. Etourneau[b]

[a]*Institute of Physics, ASCR, CZ-162 53 Praha 6, Czech Republic*
[b]*Institut de Chimie de la Matière Condensée de Bordeaux, CNRS, 33608 Pessac, France*

Received 7 July 2004; received in revised form 9 September 2004; accepted 12 September 2004
Available online 11 November 2004

Abstract

The influence of the cobalt substitution for manganese ions in the mixed valence perovskites $La_{0.8}Na_{0.2}Mn_{1-x}Co_xO_3$ ($0 \leqslant x \leqslant 0.2$) was investigated by X-ray, electric transport and magnetic measurements. The study carried out on sintered polycrystalline samples revealed the rhombohedral ($R\bar{3}c$) structure and the insulator–metal transition connected with a ferromagnetic arrangement in the whole concentration range. Increasing concentration of cobalt ions leads to a gradual decrease of PM-FM and I–M transition temperatures. An influence of the cobalt ions on the observed behavior is attributed to charge compensation $Mn^{3+} \rightarrow Mn^{4+}$ leading to the formation of stable couples Mn^{4+}–Co^{2+}. Therefore the double-exchange interactions Mn^{3+}–O^{2-}–Mn^{4+} partly vanish and they are replaced by positive superexchange interactions Mn^{4+}–O^{2-}–Co^{2+}, but of a semiconducting character.

Keywords: Manganese perovskites; Insulator–metal transition

1. Introduction

The contemporary interest about the manganites $R_{1-x}M_xMnO_3$, stimulated by their colossal magnetoresistance properties, led to the discovery of various structural and magnetic phase transitions. They occur due to an interplay of the antagonistic correlation effects, the charge ordering giving rise to an insulating antiferromagnetic arrangement and electron itinerancy inducing via double exchange mechanism the ferromagnetic metallic-type state.

Their properties are strongly influenced by the variation of the chemical composition and the following contributions should be considered:

- variation of the Mn^{3+}/Mn^{4+} ratio through the controlled valency mechanism;
- variation of the mean size of cations placed in the perovskite A sites;
- substitutions of the manganese in the perovskite *B* sites with other transition metal ions.

A large family of manganese perovskites thus exists and among them those derived from the parent compound $LaMnO_3$ possess a particular position. While $LaMnO_3$ is a single-valent (Mn^{3+}) antiferromagnetic insulator [1,2], deviations from the ideal stoichiometry or heterovalent substitutions can lead to ferromagnetism accompanied by a metallic behavior. Particular attention is devoted to the $La_{1-x}Sr_xMnO_3$ series, where replacement of lanthanum by strontium ions in the perovskite *A* sites causes a gradual decrease of the steric distortions and the structure changes from the orthorhombic (*Pbnm*) to rhombohedral ($R\bar{3}c$) symmetry. The Mn–O–Mn angles become closer to the ideal 180° arrangement and the itinerancy of e_g electrons is enhanced. It leads to a decrease of the resistivity and

*Corresponding author. Fax: +420 2 312 3184.
E-mail address: pollert@fzu.cz (E. Pollert).

0022-4596/$ - see front matter © 2004 Elsevier Inc. All rights reserved.
doi:10.1016/j.jssc.2004.09.004

Table 1
Comparison of selected lanthanum–manganese perovskites (ideal stoichiometry)

Composition	Mean r(A) (Å)	Mn^{3+} (%)	Mn^{4+} (%)	Symmetry
$La_{0.6}Ca_{0.4}MnO_3$	1.352	60	40	*Pbnm*
$La_{0.8}Na_{0.2}MnO_3$	1.366	60	40	$R\bar{3}c$
$La_{0.6}Sr_{0.4}MnO_3$	1.392	60	40	$R\bar{3}c$

I–M transition occurs for the compositions of $x > 0.17$. Simultaneously the double exchange ferromagnetic interactions are strengthened and for $x \geqslant 0.3$ a markedly high Curie temperature $T_c \sim 370$ K is achieved [3–6]. In order to understand better the role of the Mn^{3+}/Mn^{4+} ratio and steric effects it appears desirable to perform a comparative study of analogical systems. From the data in Table 1 it appears that a similar situation can be induced by replacing of La^{3+} for Na^{+}. The present study is thus focused to the compound $La_{0.8}Na_{0.2}MnO_3$ and investigates the effects of cobalt substitution for manganese ions in rhombohedral structural matrix. It is worth to mention analogous studies performed previously for the orthorhombic $Nd_{0.8}Na_{0.2}MnO_3$ and $Pr_{0.8}Na_{0.2}MnO_3$ [7,8].

2. Experimental

The samples of the compositions $La_{0.8}Na_{0.2}Mn_{1-x}Co_xO_3$ ($0 \leqslant x \leqslant 0.2$) were prepared by the conventional ceramic procedure. The compounds La_2O_3, Na_2CO_3, $MnCO_3$ and Co_3O_4 of the actual contents of the cationic components, determined by chemical analysis were homogenized in the appropriate ratios and heated at 900 °C in air for 24 h. Then the mixtures were pressed into pellets, sintered at 1100 °C under oxygen atmosphere for 96 h and subsequently quenched down to room temperature. The phase composition was checked by XRD combined with EPMA and SEM and the oxygen stoichiometry of the studied samples was determined by a redox cerimetric method. The structural refinement was performed by a profile analysis using the program FULLPROF.

The four-probe methods used for the measurements of the electrical conductivity and the thermoelectric power in the temperature range of 10–300 K are described elsewhere [9]. The DC magnetic susceptibility ($H = 100$ Oe) and the DC magnetization in fields up to 50 kOe at 10 K were measured by means of a SQUID magnetometer.

3. Results and discussion

The XRD analysis, EPMA and SEM confirmed single-phase composition of the studied samples with preserved nominal cationic ratios. A small increase of the oxygen deficiency with increasing content of cobalt ions was detected by the redox analysis. Assuming the stability of the Mn^{4+}–Co^{2+} couples [10–14] the occupancy of the octahedral sites by cations of the respective formal valencies were calculated, see Table 2.

The Rietveld refinement of X-ray diffraction data confirms rhombohedral ($R\bar{3}c$) structure for the whole concentration range. The agreement factor R_F is increasing with x from 3.7% to 4.8%. Refinement in monoclinic subgroup $I2/a$ did not improve the fit. Example of Rietveld plot for $x = 0.1$ is in Fig. 1.

The dependence of the lattice parameters on the composition plotted in Fig. 2 displays a decrease of the a parameter and an increase of the c parameter with increasing content of cobalt ions. Due to a mutual size compensation of the ions Mn^{3+}, Mn^{4+} and Co^{2+}, respectively, there is only a negligible change of the cell volume, ~0.1% from $x = 0$ to 0.2. Slight deviation for $x = 0.04$ sample from an presumed monotonous dependences is coherent with variation of the oxygen stoichiometry, see Table 2. This concept is evidenced by the comparison of the mean radii $r(Me)_B$, calculated from the data given in Table 2 and the effective ionic

Table 2
Oxygen stoichiometry and occupancy of the octahedral sites for $La_{0.8}Na_{0.2}Mn_{1-x}Co_xO_{3-\gamma}$

x	$3-\gamma$	% of cations in octahedral sites		
		Mn^{3+}	Mn^{4+}	Co^{2+}
0	2.98	64	36	0
0.04	2.98	56	40	4
0.1	2.96	48	42	10
0.2	2.92	36	44	20

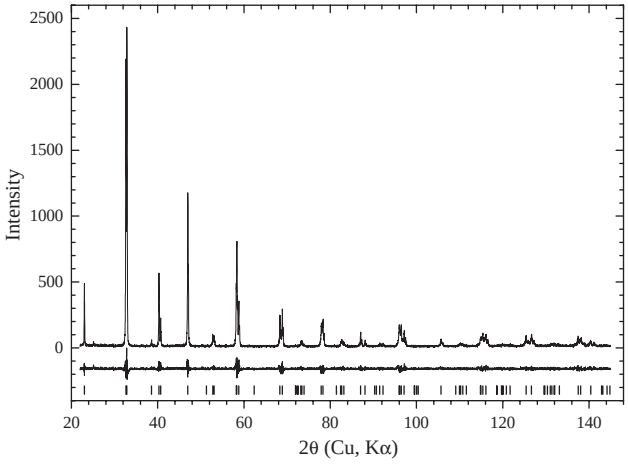

Fig. 1. An example of Rietveld X-ray diffraction plot for $x = 0.1$. Measured and difference (measured minus calculated) curves are plotted. Vertical ticks indicate the Bragg positions in $R\bar{3}c$ space group ($R_F = 4.6\%$).

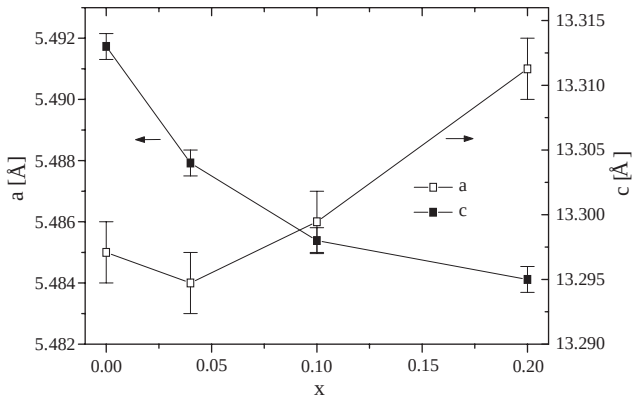

Fig. 2. Compositional dependences of the lattice parameters of $La_{0.8}Na_{0.2}Mn_{1-x}Co_xO_{3-\gamma}$ series.

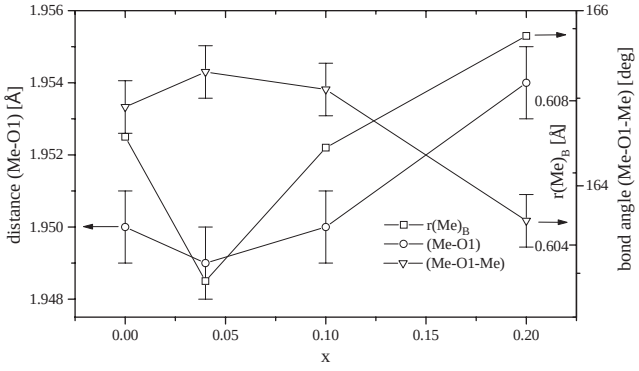

Fig. 3. Comparison of the compositional dependences of the *B*-site cations mean dimensions and of the distances (Me–O1) and of the angles (Me–O1–Me).

radii [15] with average distances (Me–O1) and average angles (Me–O1–Me) observed by X-ray diffraction, see Fig. 3. Namely, the decrease of $r(\mathrm{Me})_B$ for $x = 0.04$ is consistent with the shortening of the (Me–O1) distance and increased (Me–O1–Me) angle.

The electrical conductivities plotted in Fig. 4 show distinct anomalies that can be interpreted as the I–M transition. The critical transition temperature T_{I-M} varies from 333 K for $x = 0$ to 95 K for $x = 0.2$. In the latter case a less obvious tendency to delocalization can be seen already at ~200 K. A better insight into the conducting behavior of $x = 0.2$ is evident from the temperature dependence of the local activation energy $E_A = k_B * d(\ln \rho)/d(1/T)$, defined as a ratio of derivations of the logarithm of the electrical resistivity and reciprocal temperature, which finally becomes zero below 100 K, see the inset in Fig. 4. The discussion of the precise nature of the so-called metallic phase, given in Ref. [16] is out of the scope of the present study.

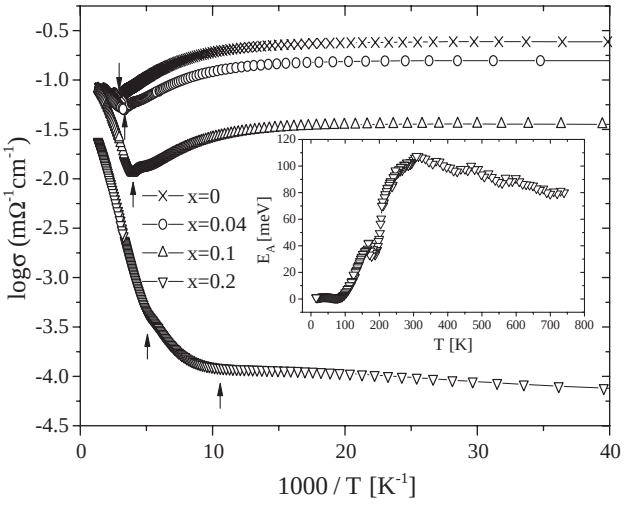

Fig. 4. Temperature dependences of the electric conductivity of $La_{0.8}Na_{0.2}Mn_{1-x}Co_xO_{3-\gamma}$ series, arrows indicate T_{I-M}.

Likewise the thermoelectric power vs. temperature dependences given in Fig. 5 demonstrate the change of the conductivity character from the n-type semiconducting to metallic one for $0 \leqslant x \leqslant 0.1$ and a more complex trend for $x = 0.2$.

The temperature dependences of the inverse magnetic susceptibility indicate clearly transition from a paramagnetic behavior to a ferromagnetic arrangement at $T < T_c$, see Fig. 6. The $M(H)$ data, (Fig. 7), measured at 10 K show a reversible FM behavior without any difference between ZFC and FC dependences and the values of the saturated magnetization are close to the theoretical ones.

In contrast to the analogous systems $Nd_{0.8}Na_{0.2}Mn_{1-x}Co_xO_3$ and $Pr_{0.8}Na_{0.2}Mn_{1-x}Co_xO_3$ the structural distortion, i.e., tilting of the octahedra, in the system $La_{0.8}Na_{0.2}Mn_{1-x}Co_xO_3$ becomes substantially lower which is crucial for the resulting magnetic and electric behavior. The average bond angles

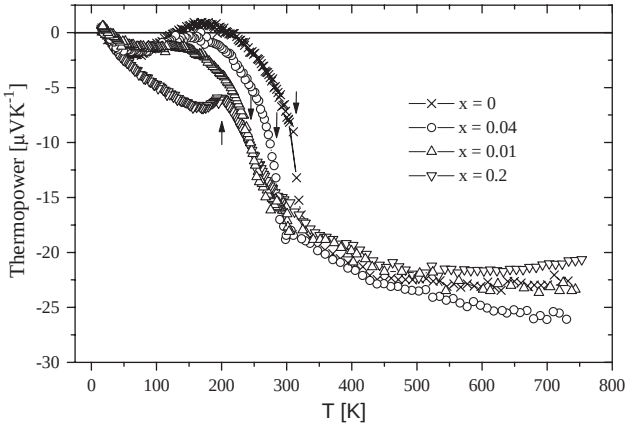

Fig. 5. Temperature dependences of the thermoelectric power of $La_{0.8}Na_{0.2}Mn_{1-x}Co_xO_{3-\gamma}$ series, arrows indicate T_{I-M}.

(Me–O1–Me) exceed the value of 160° promoting ferromagnetic double exchange interactions of the type Mn^{3+}–O^{2-}–Mn^{4+}. Upon increasing cobalt substitution, both the temperatures of PM–FM (T_c) and I–M (T_{I-M}) transitions simultaneously decrease. Particular situation appears for $x = 0.2$ where only a tendency to I–M transition is observed at $T_c = 198$ K and a metallic-like conductivity is achieved below $T \sim 95$ K. The observed behavior can be related to charge compensation $Mn^{3+} \rightarrow Mn^{4+}$ induced by Co^{2+} ions leading to the formation of Mn^{4+}–Co^{2+} couples. Consequently the double-exchange interactions Mn^{3+}–O^{2-}–Mn^{4+} partly vanish while a number of positive superexchange interactions Mn^{4+}–O^{2-}–Co^{2+}, possessing semiconducting character, increases. Evidently this effect should be strongest for $x = 0.2$, where the concentration of Co^{2+} ions is sufficiently high to hinder a tendency to I–M transition at ~200 K (Table 3).

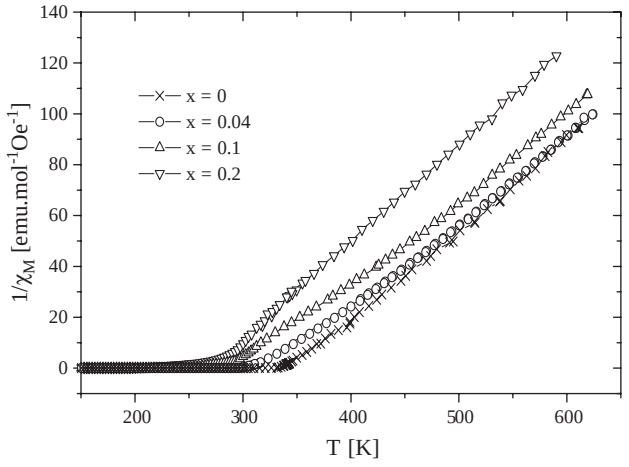

Fig. 6. Temperature dependences of the reciprocal magnetic susceptibility of $La_{0.8}Na_{0.2}Mn_{1-x}Co_xO_{3-\gamma}$ series.

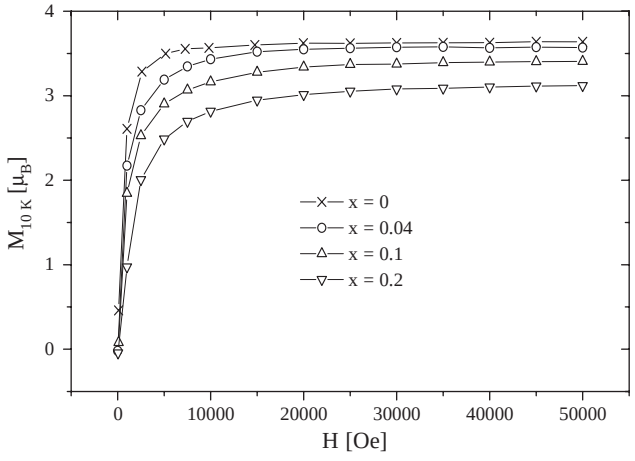

Fig. 7. Magnetic field dependences of the magnetization at 10 K of $La_{0.8}Na_{0.2}Mn_{1-x}Co_xO_{3-\gamma}$.

Very significant appear to be the thermopower data in the paramagnetic state above 300 K, that vary in a narrow range for all compositions. This nearly constant values seem to be in apparent contradiction with fast increase of Mn^{4+} concentration determined by chemical analysis. If, however, stable couples Mn^{4+}–Co^{2+} are envisaged, effective number of free hole carriers is reduced. Accordingly the variation of the hole concentration in the Mn^{3+}/Mn^{4+} array is nearly negligible, see Table 4, where the values deduced from the chemical analysis and from Seebeck coefficient data are compared.

4. Conclusion

There are two main effects decisive for the resulting magnetic and electric behavior of the $La_{0.8}Na_{0.2}Mn_{1-x}Co_xO_3$ system:

- the rhombohedral ($R\bar{3}c$) structure is preserved in the whole concentration range and tilting of the (Mn,CoO_6) octahedra is low; the average bond angles (Me–O1–Me) exceed the value of 160° promoting thus ferromagnetic double exchange interactions of the type Mn^{3+}–O^{2-}–Mn^{4+},
- substitution of cobalt for managnese ions leads to the formation of stable of Mn^{4+}–Co^{2+} couples; the double-exchange interactions Mn^{3+}–O^{2-}–Mn^{4+} are partly replaced by positive superexchange interactions Mn^{4+}–O^{2-}–Co^{2+}, possessing semiconducting character and the effective number of free hole carriers is reduced.

Table 3
Electric and magnetic data of the series $La_{0.8}Na_{0.2}Mn_{1-x}Co_xO_{3-\gamma}$

Sample	Electrical conductivity	Thermoelectric power	Magnetic constants		
x	T_{I-M} onset (K)		M_{calc} (μ_B)	M_S (10 K) (μ_B)	T_c (K)
0	333	315	3.67	3.64	325
0.04	301	286	3.56	3.6	298
0.1	255	244	3.48	3.41	246
0.2	95	—	3.22	3.16	198

Table 4
Free hole carriers in the series $La_{0.8}Na_{0.2}Mn_{1-x}Co_xO_{3-\gamma}$

x	Chemical analysis		Thermoelectric power	
	Total Mn^{4+}/Mn (%)	Free hole carriers[a] in DE Mn–O network Mn^{4+}/Mn (%)	S_{700} ($\mu V K^{-1}$)	Free hole carriers in DE Mn–O network[b] Mn^{4+}/Mn (%)
0	36	36	−23	38
0.04	42	39	−26	43
0.1	47	40	−24	40
0.2	55	40	−21	37

[a]Each cobalt ion is assumed to trap one hole; $\%[Mn^{4+}/Mn]_{DE\ Mn-O\ network} = 100\ (\%Mn^{4+} - \%Co^{2+})/(Mn^{3+} + \%Mn^{4+} - \%Co^{2+})$.
[b]Estimated using the relation between averaged high temperature thermopower data and Mn^{4+}/Mn concentration found in Refs. [9,17,18].

Acknowledgments

This study was performed under support of the Grant Agency of the Academy of Sciences of the Czech Republic (Grant A1010202).

References

[1] E.O. Wollan, W.C. Koehler, Phys. Rev. 100 (1955) 545.
[2] J.B. Goodenough, Phys. Rev. 100 (1955) 564.
[3] Y. Tokura, A. Urushibara, Y. Moritomo, T. Arima, A. Asamitsu, G. Kido, N. Furukawa, J. Phys. Soc. Jpn. 63 (1994) 3931.
[4] A. Urushibara, Y. Moritomo, T. Arima, A. Asamitsu, G. Kido, Y. Tokura, Phys. Rev. Lett. 74 (1995) 5108.
[5] A. Asamitsu, Y. Moritomo, R. Kumai, Y. Tomioka, Phys. Rev. B 54 (1996) 1716.
[6] Y. Moritomo, A. Asamitsu, Y. Tokura, Phys. Rev. B 56 (1997) 12190.
[7] E. Pollert, J. Hejtmánek, K. Knížek, M. Maryško, J.P. Doumerc, J.C. Grenier, J. Etourneau, J. Solid State Chem. 170 (2003) 368.
[8] E. Pollert, J. Hejtmánek, Z. Jirák, K. Knížek, M. Maryško, J. Solid State Chem. 174 (2003) 466.
[9] J. Hejtmánek, Z. Jirák, M. Maryško, C. Martin, A. Maignan, M. Hervieu, B. Raveau, Phys. Rev. B 63 (1999) 14057.
[10] J.H. Park, S.W. Cheong, C.T. Chen, Phys. Rev. B 55 (1997) 11072.
[11] O. Toulemonde, F. Studer, A. Barnabé, A. Maignan, C. Martin, B. Raveau, Eur. Phys. J. B 4 (1998) 159.
[12] O. Toulemonde, F. Studer, B. Raveau, Solid State Commun. 118 (2001) 107.
[13] M. Sonobe, K. Asai, J. Phys. Soc. Jpn. 61 (1992) 11.
[14] I.O. Troyanchuk, L.S. Lobanovsky, D.D. Khalyavin, S.N. Pastushonok, H. Szymczak, J. Magn. Magn. Mater. 210 (2000) 63.
[15] R.D. Shannon, Acta Crystallogr. A 32 (1976) 751.
[16] J.S. Zhou, W. Archibald, J.B. Goodenough, Nature 381 (1996) 770.
[17] J. Hejtmánek, E. Pollert, Z. Jirák, D. Sedmidubský, A. Strejc, A. Maignan, Ch. Martin, V. Hardy, R. Kuzel, Y. Tomioka, Phys. Rev. B 66 (2002) 014426.
[18] M.M. Savosta, J. Hejtmánek, Z. Jirák, M. Marysko, P. Novák, Y. Tomioka, Y. Tokura, Phys. Rev. B 61 (2000) 6896.